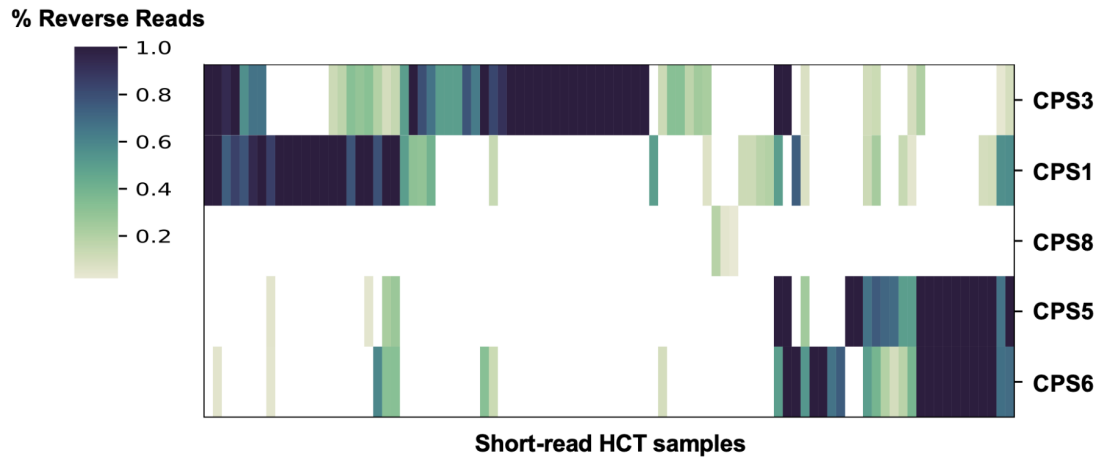


898 **Supplemental Figures**

899

900



901

902 **Fig. S1. Inversion proportion of CPS loci invertons in BTh.** Inversion proportions of CPS loci
903 invertons in HCT metagenomic samples measured with PhaseFinder. Samples with no inversions
904 in the five CPS invertons were removed.

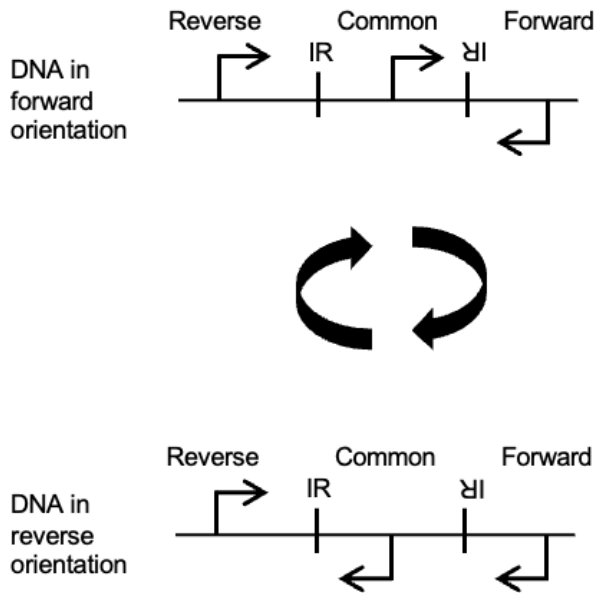
905

906

907

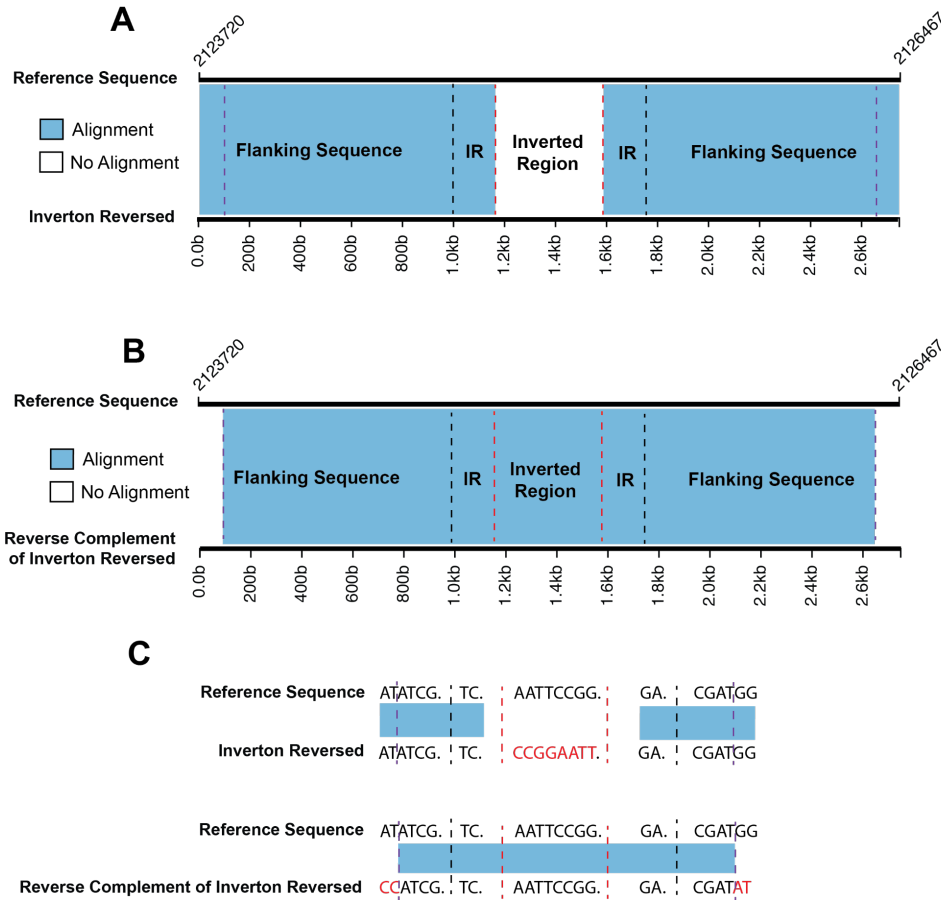
908

909



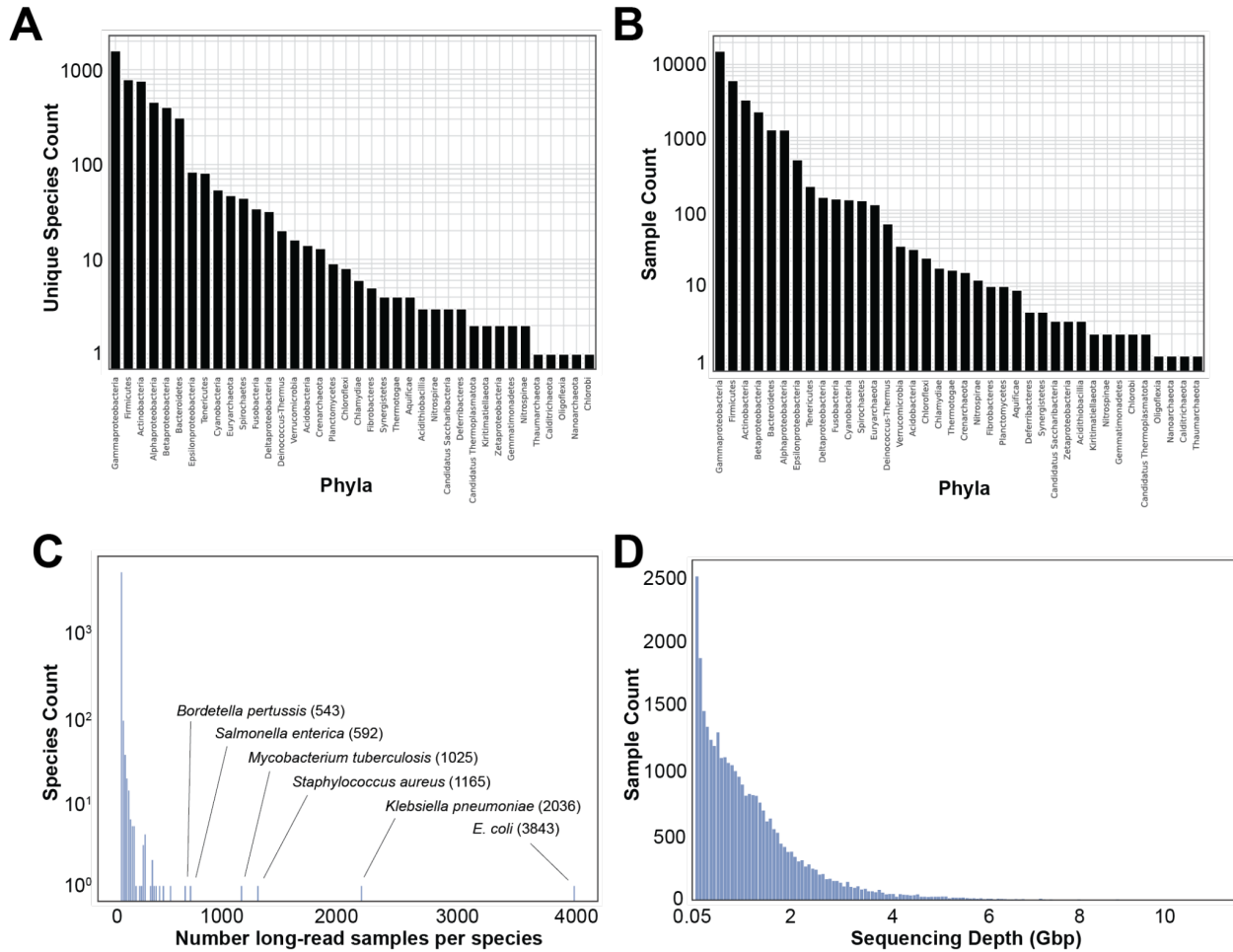
910

911 **Fig. S2. Invertion confirmation PCR primer design.** A Forward and Reverse primer bind to
912 regions of the genome upstream and downstream of the invertion on opposite strands. The
913 Common primer binds the DNA inside of the invertion, between the inverted repeats. When the
914 DNA is in the forward orientation, the Common and Forward primer will generate a PCR
915 product. When the invertion flips, the Common and Reverse primer will generate a PCR product.
916



917
918
919
920
921
922
923
924
925
926
927
928
929
930
931
932
933
934

Fig. S3. Very long (>750bp), near perfect, inverted repeats can lead to false positives. (A) Alignment of inverter NZ_CP025371.1:2124719-2124870-2125316-2125467, with its invertible sequence inverted, against the *B. pertussis* genome leads to perfect alignment of flanking and IR regions as expected. ‘Reference genome’ refers to the *B. pertussis* reference genome sequence. ‘Invertion reversed’ refers to the putative inverter sequence and flanking sequence, with the invertible sequence inverted. Red dashed lines indicate boundaries of the invertible sequence, black dashed lines indicate boundaries of the inverted repeats as detected by einverted, and purple dashed lines indicate the true boundary of inverted repeats. (B) Alignment of the reverse complement of the entire inverter NZ_CP025371.1:2124719-2124870-2125316-2125467 with its invertible sequence inverted and flanking sequence, against the *B. pertussis* genome leads to near perfect alignment (6 mismatches) spanning far into the flanking sequence to the true boundary of the inverted repeats, allowing for reads to map regardless of inverter orientation. (C) Example with toy nucleotide sequences. Red nucleotides indicate mismatches.



935

936 **Fig. S4. Overview of SRA long-read isolate sequencing samples analyzed with PhaVa. (A)**

937 The number of unique species represented in the dataset, grouped by phylum. **(B)** The raw

938 number of sequencing samples, grouped by phylum. **(C)** Histogram of sequencing samples per

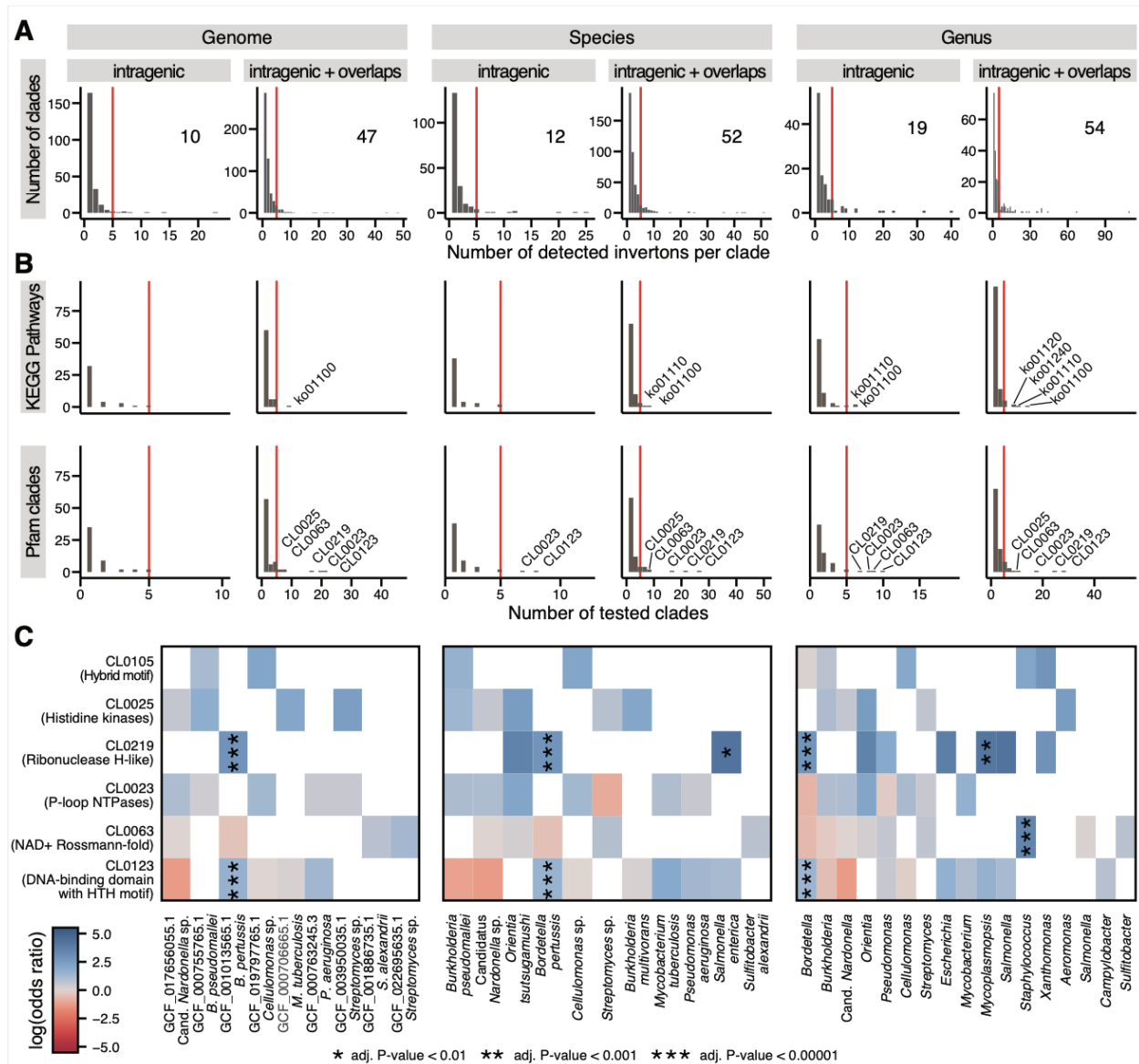
939 species. Species with particularly large numbers of samples are labeled. **(D)** A histogram of

940 sequencing depths for all long-read isolate sequencing samples.

941

942

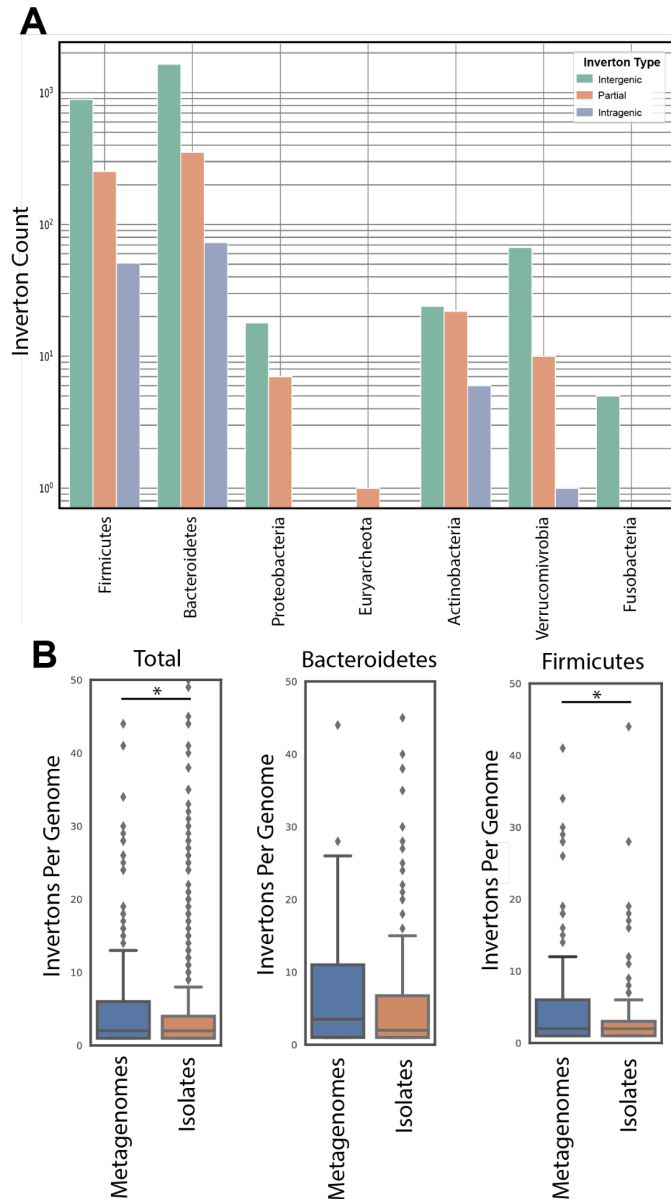
943



944

945 **Fig. S5. Intragenic invertons are rare across genomes yet consistently enriched in some**
 946 **Pfam clans. (A)** Histograms showing the number of clades (genomes, species, or genera) at
 947 various numbers of invertons indicate that invertons are rare, as only one to three
 948 invertons can be detected in the majority of clades. Only clades with at least five
 949 invertons (red line; number of clades is indicated in the top-right corner of each
 950 subplot) were included for the subsequent enrichment analysis. **(B)** KEGG pathways
 951 and Pfam clans were tested for enrichment of intragenic (or partial intergenic)
 952 invertons in included clades, using a one-sided Fisher's exact test per clade (see
 953 Methods). Enrichment was only calculated for sets with at least five invertons
 954 associated with genes in the set. Histograms show the number of sets with enrichment
 score at the number of included clades, showing that most enrichments could be
 calculated for single

955 clades only. For example, all KEGG pathways associated with enough intragenic invertons for
956 an enrichment analysis on genome-level were specific for each genome. Sets with enrichment
957 scores across at least five clades (red line) are labeled with their corresponding identifiers. **(C)**
958 Heatmap showing the log-odds ratio (effect size for the enrichment of intragenic invertons)
959 across included clades for the six Pfam clans that have enrichment scores on genus-level (see
960 panel B). Stars indicate significance of the enrichment as calculated by Fisher's exact test and
961 corrected for multiple hypothesis testing using the Benjamini-Hochberg procedure.
962

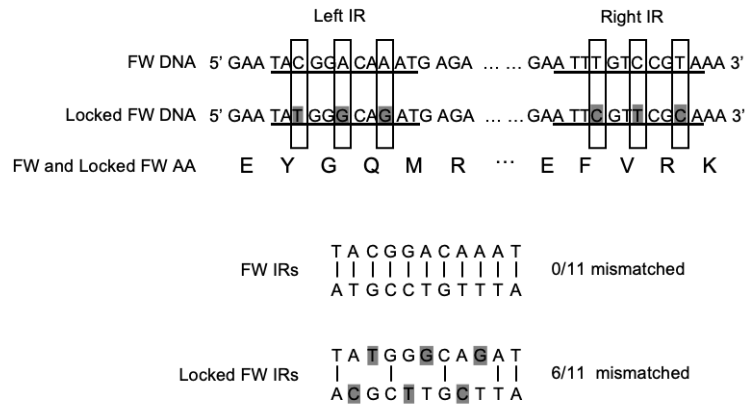


963

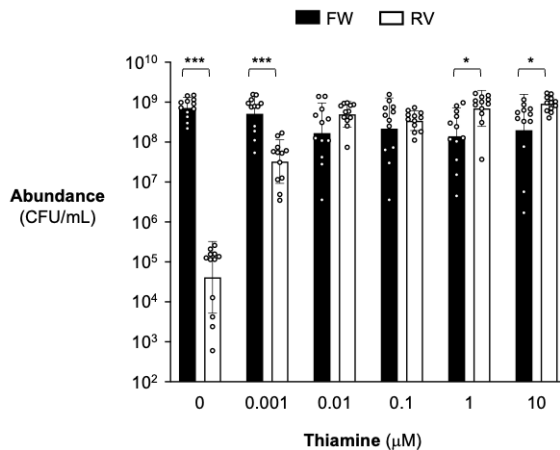
964 **Fig. S6. PhaVa analysis of 210 long-read metagenomes from human stool.** (A) Counts of
965 invertions identified with PhaVa in 210 stool samples, grouped by phylum and the type of
966 invertion. (B) Comparisons of the number of invertions (per genome) found in metagenomic
967 datasets vs. SRA isolate sequencing samples. Total refers to all invertions identified, regardless of
968 taxonomic classification. The distribution of invertion counts per species were found to be
969 significantly different between metagenomes and isolate samples in both the Total and
970 Firmicutes comparisons ($p=3.35e-05$ and $p=0.005$ respectively) with a Kolmogorov–Smirnov
971 test. Other individual phyla were not compared due to small species counts with invertions in
972 metagenomic samples.

973

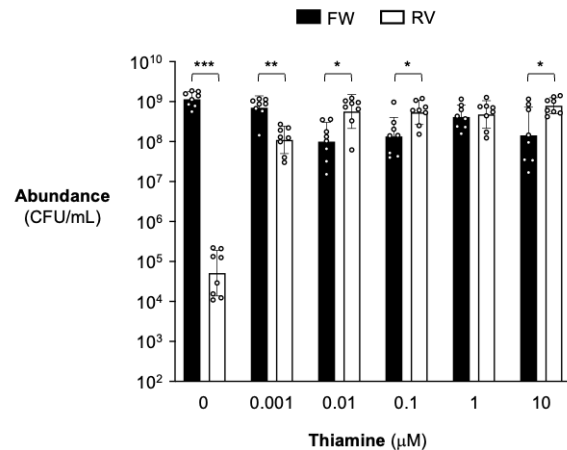
A



B



C

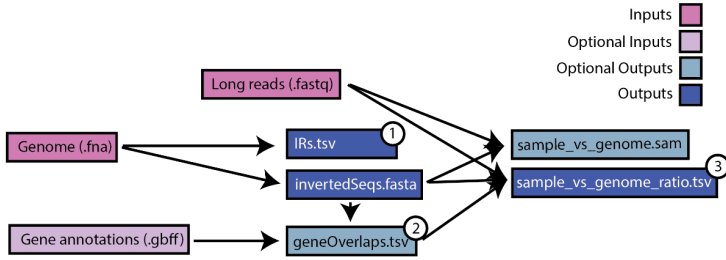


974

975 **Fig. S7. Locked *thiC* intragenic inverton construction and growth competition. (A)**
976 Generation of locked intragenic invertons. The forward and locked forward *thiC* IR nucleotide
977 sequences are shown. When possible, the wobble position of each codon corresponding to the IR
978 was mutated to increase mismatches between the two palindromic sequences while maintaining
979 the amino acid sequence. Nucleotides that were mutated are highlighted in gray. **(B-C)** Locked
980 *thiC* strains were competed against each other in thiamine-containing media in a 1:1 ratio. After
981 40 hours, the abundance of each strain was enumerated using selective agar. Black bars indicate
982 the locked forward strain and white bars indicate the locked reverse strain. Recovered
983 abundances shown here correspond with the competitive index shown in Fig. 4D. In **(B)** the
984 locked forward strain is marked with an erythromycin resistant cassette and the locked reverse
985 strain is marked with a tetracycline resistant cassette. In **(C)** the locked forward strain is marked
986 with a tetracycline resistant cassette and the locked reverse strain is marked with an
987 erythromycin resistant cassette. Geometric mean and geometric standard deviation are shown for
988 replicates conducted across 4-6 independent experiments. For each thiamine concentration a ratio
989 paired t test was performed on the locked forward and locked reverse abundances. ***, $p <$
990 0.001; **, $p <$ 0.01; *, $p <$ 0.05.

991

992



① IRs.tsv

chromosome	left IR start	left IR stop	right IR start	right IR stop	left IR sequence	invertible sequence	right IR sequence
chr1	1032	1046	1146	1160	ATCG	TACGGATATTACG	CGAT

② geneOverlaps.tsv

Invertion	gene overlaps	Upstream Gene	Upstream Gene	Upstream Gene	Downstream Gene	Downstream Gene	Downstream Gene
		Strand	Distance		Strand	Distance	
inv1	intragenic BT04	BT03	+	100	BT05	-	150

③ sample_vs_genome_ratio.tsv

Invertion	gene overlaps	forward read #	reverse read #	reverse ratio	sample	Upstream Gene	Upstream Gene	Upstream Gene	Downstream Gene	Downstream Gene	Downstream Gene
						Strand	Distance		Strand	Distance	
inv1	intragenic BT04	15	5	0.25	SRR123	BT03	+	100	BT05	-	150

993

994 **Figure S8: Inputs and outputs of a variation_wf PhaVa run.** Output tables of particular
 995 interest are labeled and shown below the diagram with example output.

Strain name	Source	Identifier
<i>Bacteroides thetaiotaomicron</i> VPI-5482 Δtdk	⁷⁹	WT
<i>Bacteroides thetaiotaomicron</i> VPI-5482 Δtdk $\Delta BT0650$	this study	RC131
<i>Bacteroides thetaiotaomicron</i> VPI-5482 Δtdk BT0650 locked RV	this study	RC149
<i>Bacteroides thetaiotaomicron</i> VPI-5482 Δtdk BT0650 locked FW	this study	RC134
<i>Bacteroides thetaiotaomicron</i> VPI-5482 Δtdk BT0650 locked FW <i>NBU2::NBU2_tet</i>	this study	RC165
<i>Bacteroides thetaiotaomicron</i> VPI-5482 Δtdk BT0650 locked FW <i>NBU2::NBU2_erm</i>	this study	RC 166
<i>Bacteroides thetaiotaomicron</i> VPI-5482 Δtdk BT0650 locked RV <i>NBU2::NBU2_erm</i>	this study	RC164
<i>Bacteroides thetaiotaomicron</i> VPI-5482 Δtdk BT0650 locked RV <i>NBU2::NBU2_tet</i>	this study	RC163
<i>E. coli</i> S17-1 λpir ; <i>zxx::RP4 2-(Tetr::Mu) (Kanr::Tn7) \lambda pir</i>	⁸⁰	S17-1 λpir
<i>E. coli</i> DH5 α λpir ; <i>F- endA1 hsdR17 (r-m+) supE44 thi-1 recA1 gyrA relA1 \Delta(lacZYA-argF)U189 \phi80lacZ\Delta M15 \lambda pir</i>	⁸¹	DH5 α λpir

996
997
998

Table S1. Strains used in this study

Recombinant DNA	Identifier	Source
pKNOCK- <i>bla-ermGb::tdk</i>	pExchange	79
pExchange BT0650 KO	pRBC20	this study
pExchange BT0650 locked FW	pRBC21	this study
pExchange BT0650 locked RV	pRBC22	this study
pNBU2_tet	tetR	24
pNBU2_erm	ermR	24

999
1000
1001

Table S2. Recombinant DNA used in this study